19. The choice of orientation for knots is arbitrary. The paths assigned to catenated rings formed by recombination must reflect a common orientation of the parental circle. For catenanes not formed by recombination, the orientations of the two rings should, where possible, reflect common asymmetric sequence.
20. D. Rolfsen, *Knots and Links* (Publish or Perish, Inc., Wilmington, DE, 1976).
21. J. H. White and N. R. Cozzarelli, *Proc. Natl. Acad. Sci. U.S.A.* **81**, 3322 (1984).
22. W. Keller, *ibid.* **72**, 8476 (1975).
23. F. B. Dean, A. Stasiak, Th. Koller, N. R. Cozzarelli, *J. Biol. Chem.* **260**, 4975 (1985).
24. O. Sundin and A. Varshavsky, *Cell* **21**, 103 (1980); *ibid.* **25**, 659 (1981).
25. H. W. Benjamin, M. M. Matzuk, M. A. Krasnow, N. R. Cozzarelli, *ibid.* **40**, 147 (1984).
26. S. A. Wasserman, J. M. Dungan, N. R. Cozzarelli, *Science* **229**, 171 (1985).
27. L. F. Liu, R. E. Depew, J. C. Wang, *J. Biol. Chem.* **106**, 439 (1976); R. A. Fishel and R. C. Warner, *Virology* **148**, 198 (1986).
28. M. A. Krasnow *et al.*, *Nature (London)* **304**, 559 (1983).
29. J. Griffith and H. A. Nash, *Proc. Natl. Acad. Sci. U.S.A.* **82**, 3124 (1985).
30. J. C. Wang and H. Schwartz, *Biopolymers* **5**, 953 (1967).
31. B. Hudson and J. Vinograd, *Nature (London)* **216**, 647 (1967); D. A. Clayton and J. Vinograd, *ibid.*, p. 652; R. Radloff, W. Bauer, J. Vinograd, *Proc. Natl. Acad. Sci. U.S.A.* **57**, 1514 (1967).
32. W. Goebel and D. R. Helinski, *Proc. Natl. Acad. Sci. U.S.A.* **61**, 1406 (1968); G. Riou and E. Delain, *ibid.* **62**, 210 (1969); R. Jaenisch and A. J. Levine, *Virology* **44**, 480 (1971); H. C. Macgregor and M. Vlad, *Chromosoma* **39**, 205 (1972).
33. W. Meinke and D. A. Goldstein, *J. Mol. Biol.* **61**, 543 (1971).
34. J. M. Sogo, M. Greenstein, A. Skalka, *J. Biol. Chem.* **103**, 537 (1976).
35. M. L. Gefter, *Annu. Rev. Biochem.* **44**, 45 (1975).
36. J. Cairns, *J. Mol. Biol.* **6**, 208 (1963).
37. J. J. Champoux and M. D. Been, in *Mechanistic Studies of DNA Replication and Genetic Recombination*, B. Alberts, Ed. (Academic Press, New York, 1980), p. 809.
38. W. F. Pohl and G. W. Roberts, *J. Math. Biol.* **6**, 383 (1978).
39. Y. Tse and J. C. Wang, *Cell* **22**, 269 (1980); P. O. Brown and N. R. Cozzarelli, *Proc. Natl. Acad. Sci. U.S.A.* **78**, 843 (1981); R. L. Low, J. M. Kaguni, A. Kornberg, *J. Biol. Chem.* **259**, 4576 (1984); K. J. Marians, personal communication.
40. A. Varshavsky *et al.*, in *Mechanisms of DNA Replication and Recombination*, N. R. Cozzarelli, Ed. (Liss, New York, 1983), vol. 10, p. 463.
41. D. T. Weaver, S. C. Fields-Berry, M. L. DePamphilis, *Cell* **41**, 565 (1985).
42. S. DiNardo, K. Voelkel, R. Sternglanz, *Proc. Natl. Acad. Sci. U.S.A.* **81**, 2616 (1984); C. Thrash, A. T. Bankier, B. G. Barrell, R. Sternglanz, *J. Biol. Chem.* **259**, 1375 (1984).
43. C. Holm, T. Goto, J. C. Wang, D. Botstein, *Cell* **41**, 553 (1985).
44. G. O. Stonington and D. E. Pettijohn, *Proc. Natl. Acad. Sci. U.S.A.* **68**, 6 (1971); A. Worcel and E. Burgi, *J. Mol. Biol.* **71**, 127 (1972); C. Benyajati and A. Worcel, *Cell* **9**, 393 (1976); J. R. Paulson and U. K. Laemmli, *ibid.* **12**, 817 (1977).
45. T. Uemura and M. Yanagida, *EMBO J.* **3**, 1737 (1984).
46. Y. Sakakibara, K. Suzuki, J. I. Tomizawa, *J. Mol. Biol.* **108**, 569 (1976); M. S. Wold, J. B. Mallory, J. D. Roberts, J. H. LeBowitz, R. McMacken, *Proc. Natl. Acad. Sci. U.S.A.* **79**, 6176 (1982); J. S. Minden and K. J. Marians, personal communication.
47. T. R. Steck and K. Drlica, *Cell* **36**, 1081 (1984).
48. J. Bliska and N. R. Cozzarelli, unpublished results.
49. M. A. Krasnow and N. R. Cozzarelli, *J. Biol. Chem.* **257**, 2687 (1982).
50. A. Stasiak, M. A. Krasnow, N. R. Cozzarelli, unpublished observations.
51. H. A. Nash, *Annu. Rev. Genet.* **15**, 143 (1981); R. Weisberg and A. Landy, in *Lambda II*, R. W. Hendrix, J. W. Roberts, F. W. Stahl, R. A. Weisberg, Eds. (Cold Spring Harbor Laboratory, Cold Spring Harbor, NY, 1983), p. 211.
52. F. Heffron, in *Mobile Genetic Elements*, J. A. Shapiro, Ed. (Academic Press, New York, 1983), p. 223; N. D. F. Grindley and R. Reed, *Annu. Rev. Biochem.* **54**, 863 (1985).
53. R. R. Reed, *Cell* **25**, 713 (1981).
54. M. A. Krasnow, M. M. Matzuk, J. M. Dungan, H. W. Benjamin, N. R. Cozzarelli, in *Mechanisms of DNA Replication and Recombination*, N. R. Cozzarelli, Ed. (Liss, New York, 1983), p. 637; H. W. Benjamin and N. R. Cozzarelli, in *Welch Symposium 1985*, in press.
55. N. D. F. Grindley *et al.*, *Cell* **30**, 19 (1982); R. G. Wells and N. D. F. Grindley, *J. Mol. Biol.* **179**, 667 (1984).
56. J. Salvo and N. D. F. Grindley, unpublished results.
57. H. W. Benjamin and N. R. Cozzarelli, unpublished results.
58. M. Better, C. Lu, R. C. Williams, H. Echols, *Proc. Natl. Acad. Sci. U.S.A.* **79**, 5837 (1982); H. Echols, *BioEssays* **1**, 148 (1984).
59. K. Mizuuchi, M. Gellert, R. A. Weisberg, H. A. Nash, *J. Mol. Biol.* **141**, 485 (1980).
60. N. L. Craig and H. A. Nash, in *Mechanisms of DNA Replication and Recombination*, N. R. Cozzarelli, Ed. (Liss, New York, 1983), vol. 10, p. 617.
61. H. A. Nash and T. J. Pollock, *J. Mol. Biol.* **170**, 19 (1983); T. J. Pollock and H. A. Nash, *ibid.*, p. 1.
62. S. Yin, W. Bushman, A. Landy, *Proc. Natl. Acad. Sci. U.S.A.* **82**, 1040 (1985).
63. T. J. Pollock and K. Abremski, *J. Mol. Biol.* **131**, 651 (1979).
64. D. W. Sumners, personal communication.
65. J. H. Wilson, *Proc. Natl. Acad. Sci. U.S.A.* **76**, 3641 (1979); S. McGavin, *J. Mol. Biol.* **55**, 293 (1971).
66. S. A. Wasserman and N. R. Cozzarelli, unpublished results.
67. M. Bianchi, C. DasGupta, C. M. Radding, *Cell* **34**, 931 (1983).
68. We thank E. Blackburn, M. Botchan, H. Echols, H. Nash, R. Sternglanz, J. Wang, and especially Alex Varshavsky and Mark Krasnow for their critical reading of the manuscript. Supported in part by NIH grants GM31655 and 31657 to N.R.C. and by a grant from the Lucille P. Markey Charitable Trust to S.A.W.

Two-Dimensional Nuclear Magnetic Resonance Spectroscopy

AD BAX AND LAURA LERNER

Great spectral simplification can be obtained by spreading the conventional one-dimensional nuclear magnetic resonance (NMR) spectrum in two independent frequency dimensions. This so-called two-dimensional NMR spectroscopy removes spectral overlap, facilitates spectral assignment, and provides a wealth of additional information. For example, conformational information related to interproton distances is available from resonance intensities in certain types of two-dimensional experiments. Another method generates ^{1}H NMR spectra of a preselected fragment of the molecule, suppressing resonances from other regions and greatly simplifying spectral appearance. Two-dimensional NMR spectroscopy can also be applied to the study of ^{13}C and ^{15}N, not only providing valuable connectivity information but also improving sensitivity of ^{13}C and ^{15}N detection by up to two orders of magnitude.

SINCE ITS DISCOVERY 40 YEARS AGO, NUCLEAR MAGNETIC resonance (NMR) spectroscopy has evolved continuously, becoming a powerful technique for studying molecular structures and interactions. In this article we describe a major development, two-dimensional Fourier transform pulse NMR (2-D FT NMR), which has extended the range of applications of NMR spectroscopy, particularly with respect to large, complex molecules such as DNA and proteins.

Jeener (*1*) first introduced the concept of 2-D FT NMR in 1971. This original experiment was analyzed in detail by Aue *et al.* (*2*) in a paper that provided the basis for the development of a tremendous number of new pulse sequences. One important application of the 2-D FT approach in NMR, suggested by Ernst and co-workers (*3*), is in magnetic resonance imaging (a new tool in diagnostic medicine), where it now has largely replaced the earlier projection-reconstruc-

The authors are in the Laboratory of Chemical Physics, National Institute of Arthritis, Diabetes and Digestive and Kidney Diseases, National Institutes of Health, Bethesda, MD 20892.

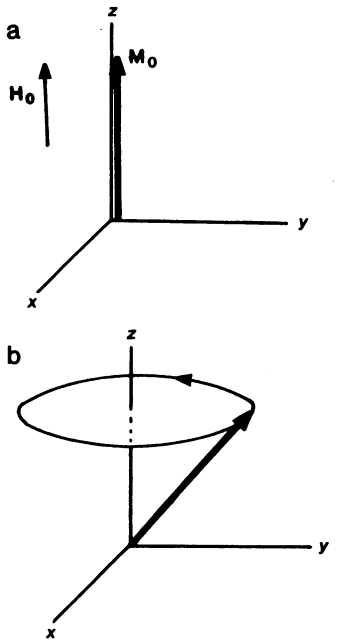

Fig. 1. Vector picture of NMR. (a) At equilibrium, the magnetization vector, M_0, is aligned along the static magnetic field, H_0. (b) The application of an RF pulse rotates this magnetization away from the z axis, after which it precesses with its resonance frequency about the z axis.

tion NMR method (*4*). Early chemical applications of 2-D methods focused on the separation of chemical shift and scalar coupling effects along the two frequency axes of a 2-D spectrum, in order to simplify analysis of overlapping spectral lines (*5*).

Although several hundred different 2-D pulse sequences have been published, most of these are variations on a common theme: observation of the transfer of magnetization from one nucleus to another. No comprehensive and critical review covering the field has appeared to date, but some introductory literature is available (*6*).

Principles of 2-D FT NMR

To begin to explain 2-D FT NMR, we review the essential features of the one-dimensional (1-D) pulse NMR experiment. Although NMR is a quantum mechanical phenomenon, much insight can be gained by using a vector picture based on the classic Bloch equations (*7*). In this vector picture, the macroscopic nuclear magnetization (M_0) at thermal equilibrium is aligned parallel to the static magnetic field, which is chosen parallel to the z axis of our coordinate system (Fig. 1a). A radio-frequency (RF) pulse is applied to rotate the magnetization away from the z axis; after the pulse is turned off, the magnetization will precess at the resonance (Larmor) frequency about the z axis (Fig. 1b). Typical resonance frequencies range from 10 to 500 MHz, depending on the static magnetic field strength used and on the gyromagnetic ratio, γ, of the nucleus. For example, at the highest field strength commercially available, 11.75 tesla, ^{1}H precesses at 500 MHz, ^{31}P at 202 MHz, ^{13}C at 125 MHz, and ^{15}N at 50 MHz. In practice, it is convenient to monitor the magnetization in a reference frame that rotates with the frequency of the RF pulse transmitter about the z axis. This carrier frequency is chosen to be within several kilohertz from the resonance frequencies of interest. By the application of a pulse, the magnetization can be rotated through arbitrary angles about the x or y axis of the rotating reference frame. After the RF pulse is turned off, the magnetization precesses about the z axis of the rotating frame at the offset frequency of the RF pulse, which equals the difference between the resonance and the carrier frequencies. The spectrometer observes the signal that is induced in the detection coil by this precessing xy magnetization. This signal does not persist indefinitely, but decays with time as a result of relaxation processes and thus is called the free induction decay or FID. The observed FID is digitized and stored in computer memory. A Fourier transformation of this signal results in a spectrum with resonance lines at the offset frequencies corresponding to each nucleus observed. Only magnetization of nuclei whose frequencies fall within a narrow band (usually about ±25 kHz) around the carrier frequency of the RF pulse can be rotated and observed by the application of a single pulse, and hence, only one type of nucleus is detected at a time.

At a constant field strength, the resonance frequency of a particular nucleus depends on its chemical environment. This relatively small chemical shift effect (usually expressed in parts per million or ppm) is the main reason why an NMR spectrum contains such an abundance of detail about chemical structure. This detail can be used if each resonance line can be assigned to its corresponding nucleus. The power of 2-D NMR lies in its ability to resolve overlapping spectral lines, to enhance sensitivity, and to provide information not available by 1-D methods. In addition, 2-D NMR has made it feasible to measure internuclear distances and scalar coupling constants in molecules that are too complex for a 1-D approach.

A typical 2-D pulse sequence is shown schematically in Fig. 2a. The two frequency dimensions of 2-D NMR originate from the two time intervals, t_1 and t_2, during which the nuclei can be subjected to two different sets of conditions. The amplitude of the signals detected during time t_2 is a function of what happened to the nuclei during the evolution period, t_1. If the experiment is repeated for a large number of incremented t_1 durations, varying from 0 to several hundred milliseconds, a set of spectra is obtained with the amplitude of the resonances modulated with the frequencies that existed during the evolution period, t_1. A Fourier transformation with respect to t_1 defines the modulation frequencies and results in a 2-D spectrum.

The procedure described above will be illustrated in some detail for the pulse sequence of Fig. 2a that is applied to the three methyl resonances in *N,N*-dimethylacetamide (Fig. 3). The two methyl groups, labeled A and B in Fig. 3a, directly attached to the nitrogen are nonequivalent and in slow exchange. We will concentrate on what happens to the magnetization of A during the experiment to demonstrate how a 2-D pulse sequence can be used to observe this exchange. The first 90° pulse applied along the x axis of the rotating frame (designated a 90°$_x$ pulse) rotates the A magnetization from the z to the y axis (Fig. 2b). After this pulse, the transverse A magnetization will precess freely with its offset frequency, Ω_A, about the static magnetic field (the z axis). At time t_1, this magnetization vector has covered an angle $\theta = \Omega_A t_1$ (Fig. 2c). The second 90°$_x$ pulse then rotates the magnetization vector into the zx plane. Just after this pulse, the x and z components of this magnetization are proportional to $\sin(\Omega_A t_1)$ and $-\cos(\Omega_A t_1)$, respectively. The x component can be eliminated by temporarily applying a small gradient on the static magnetic field, so that only magnetization parallel to the z axis remains. If after a mixing time, Δ, the amount of z magnetization is observed by means of another 90° pulse, then the intensity of resonance A will be proportional to $\cos(\Omega_A t_1)$ (Fig. 3a). However, if some of the A and B methyl groups have interchanged their position (and their chemical shift), a fraction of the B resonance will also be modulated in amplitude by $\cos(\Omega_A t_1)$. For the same reason, a similar fraction of the A resonance will be modulated by $\cos(\Omega_B t_1)$. Fourier transformation of sections parallel to the t_1 axis of the data matrix of Fig. 3a measures these modulation frequencies and results in the 2-D spectrum of Fig. 3b. For practical reasons, this spectrum is usually displayed as a contour plot (Fig. 3c). The so-called cross peaks, at coordinates $(\omega_1,\omega_2) = (\Omega_B,\Omega_A)$ and (Ω_A,Ω_B), represent magnetization that has changed its precession frequency between the evolution and detection periods. By measuring the intensity of the cross peak relative to the diagonal

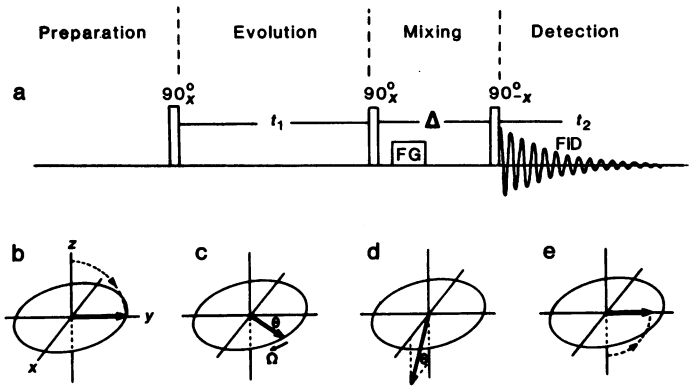

Fig. 2. (a) Example of a 2-D NMR pulse sequence. The experiment is repeated for a large number of incremental t_1 durations, yielding a 2-D time domain signal, $s(t_1,t_2)$. Magnetization vector picture, (b) just after the first 90°$_x$ pulse, (c) just before the second 90°$_x$ pulse, (d) just after the second 90°$_x$ pulse, and (e) just after the final 90° pulse, applied along the $-x$ axis. The xy magnetization present after the second 90°$_x$ pulse is removed by the application of a magnetic field gradient (FG). More commonly, a procedure referred to as phase cycling is used to eliminate xy magnetization. FID, free induction decay.

peak (on a diagonal line from Ω_A,Ω_A through Ω_C,Ω_C) one can calculate the exchange rate (*8, 8a*).

In the example discussed above, magnetization was transferred from one resonance to the other by chemical exchange. It is also possible to transfer magnetization from nucleus A to nucleus B by the nuclear Overhauser effect (NOE) or through the scalar-coupling (*J* coupling) mechanism. Practical applications of these experiments are discussed below. Most commonly, nuclei A and B are both protons, or ^{1}H and ^{13}C nuclei, although a large number of other combinations have been explored successfully. In other experiments the physical environment of the spin system is different for the evolution and detection periods. For example, irradiation (decoupling) of nonobserved nuclei coupled to observed nuclei is switched on or off between evolution and detection periods (*5*) or, in solids, the orientation of the sample may be changed (*9*). A large number of other variations are also possible. Some of the standard and more advanced experiments that demonstrate the power of the 2-D approach are discussed below.

Two-Dimensional NOE Spectroscopy

The 2-D technique for measuring homonuclear (^{1}H-^{1}H) NOE effects, proposed by Jeener, Ernst, and co-workers (*8*), is a powerful tool for obtaining conformational information for molecules with molecular weights up to 15,000.

The NOE effect causes the intensity of the resonance of nucleus A to change if the z component of the magnetization of a nearby nucleus X is perturbed. This is caused by an interaction between the magnetic dipole moments of the two nuclei (*10*). For protons, a good approximation of the initial rate of intensity change observed for nucleus A on perturbation of the z magnetization of X is given by:

$$k = [34.2\tau_c/(1 + 4\omega^2\tau_c^2) - 5.7\tau_c] \times 10^{10} r^{-6} \quad (1)$$

where r is the distance between protons A and X (in angstroms), ω is the angular proton resonance frequency, and τ_c is the correlation time of the molecule (approximately the time it takes the molecule to tumble, on average, through an angle of 1 radian). This expression shows that the NOE buildup rate, k, is proportional to r^{-6}, and that measurement of k directly determines the interproton distance, r, if τ_c is known. If τ_c is not known, one uses two protons at a known distance r_0 (for example, vicinal aromatic protons or two geminal protons) as an internal reference. If NOE's build up at rates k_0 for the reference protons and k for the AX pair of interest, then the distance between A and X equals $(k_0/k)^{1/6} r_0$.

The NOE effect has been known for a long time and has been used extensively in 1-D homonuclear NOE measurements. In these experiments the magnetization of one nucleus is perturbed selectively by irradiation with a weak RF field, and the changes in the intensities of other resonances in the spectrum are then monitored. If one measures distances among a large number of different protons, an equally large number of such 1-D experiments are needed. Moreover, in complex proton spectra, a truly selective perturbation is often impossible because of spectral overlap. As will be shown below, the 2-D NOE experiment overcomes these two problems by measuring all interproton distances simultaneously and by spreading the overlapping spectrum in two frequency dimensions.

The pulse sequence of this so-called NOESY (NOE SpectroscopY) experiment is the same as for the 2-D exchange experiment discussed earlier (Fig. 2a) and the analysis is almost identical. Using

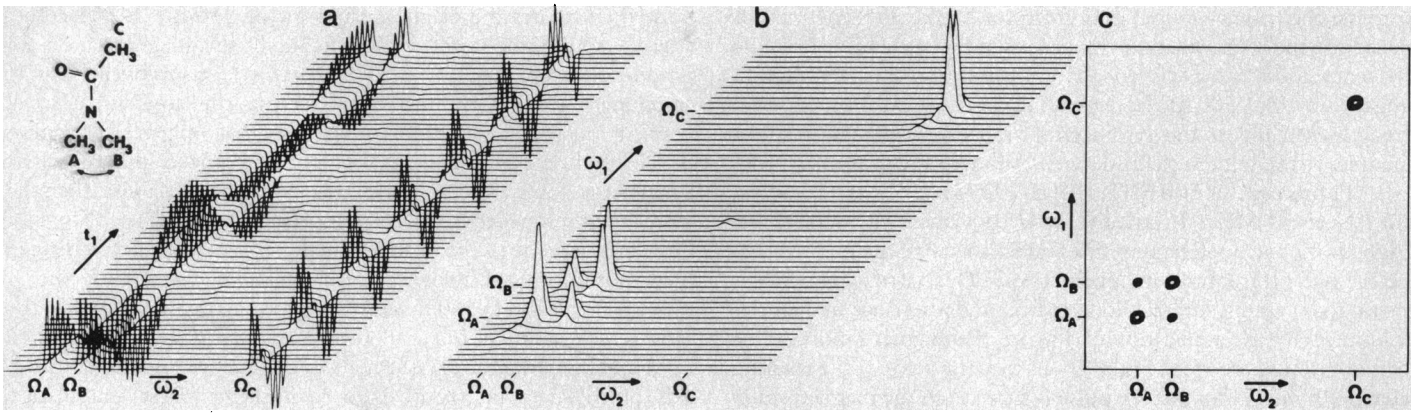

Fig. 3. The generation of a 2-D exchange spectrum of *N,N*-dimethylacetamide, from data obtained with the pulse sequence of Fig. 2a (the mixing time was 500 msec). After Fourier transformation with respect to t_2, a set of spectra modulated in amplitude as a function of t_1 is obtained (a). A Fourier transformation, with respect to t_1, of the columns of the data matrix corresponding to this set of spectra yields resonances at the modulation frequencies in this dimension. This is the final 2-D spectrum (b). For clarity, this spectrum is often displayed as a contour plot (c). The cross peak at (Ω_A,Ω_B) represents methyl protons that have changed their position (and hence resonance frequency) from A to B. Peaks on the diagonal represent protons that have not changed their resonance frequency during the mixing period.

the same vector description, we see that at the beginning of the mixing time Δ, the z component of the magnetization of nucleus A is proportional to $-\cos(\Omega_A t_1)$. The deviation from thermal equilibrium of the z magnetization of proton A is transferred by the NOE effect to nuclei that have a significant dipolar interaction with A. Hence, if X is close in space to A ($r < 5$ Å), the z magnetization of X will depend on, among other factors, $\cos(\Omega_A t_1)$. The X magnetization monitored after the final 90°$_x$ pulse will thus show a modulation by $\cos(\Omega_A t_1)$, and a 2-D Fourier transformation will show a corresponding resonance at coordinates $(\omega_1,\omega_2) = (\Omega_A,\Omega_X)$, indicating that dipolar cross relaxation (the NOE effect) has occurred during time Δ. The intensity of such an off-diagonal resonance in the 2-D spectrum depends on k (Eq. 1); that is, on r^{-6}, on τ_c, and on time Δ. For small molecules, rapid tumbling corresponds to small τ_c values ($<10^{-10}$second) and correspondingly small k values. Hence, a relatively long mixing time Δ on the order of the longitudinal relaxation time T_1 is necessary to obtain cross peaks of substantial intensity. For macromolecules ($\tau_c > 5 \times 10^{-9}$ second) the NOE effect builds up rapidly and short Δ values (25 to 300 msec) can be used.

As an example, Fig. 4 shows the 2-D NOE spectrum of a DNA oligomer of 17 base pairs (*11*). For comparison, the conventional 1-D spectrum of this macromolecule is also presented. Although only a few of the approximately 300 proton resonances in the 1-D spectrum are properly resolved, in the 2-D spectrum most of this overlap is removed. Moreover, the intensity of each of the approximately 300 resolvable off-diagonal resonances in the 2-D spectrum corresponds to an interproton distance. Assuming that the molecule is in a right-handed B-DNA–type helix conformation, resonance assignments follow from the 2-D NOE spectrum in a straightforward manner (*12*), despite the complexity of the contour plot. Refinements to the structure can then be made by quantifying the NOE cross-peak intensities. If the molecule had been in a quite different conformation (for example, A-DNA or Z-DNA), it would have yielded a distinctly different pattern of cross peaks (*13*). Observation of the solution structure of DNA fragments by 2-D NOESY is becoming routine (*14*). Since spectra can be obtained on samples in solution under physiologically relevant conditions, NMR may offer advantages over x-ray crystallography, which requires relatively dehydrated crystals or fibers as samples.

The use of 2-D NOESY for structure determination is, of course, not limited to nucleic acids. Pioneering efforts by Wüthrich, Wagner, and co-workers (*15*) to apply the method to proteins have been successful, and a number of impressive applications have now been reported (*16*). It appears possible to determine the entire 3-D structure of small proteins without reference to x-ray crystallographic data. In addition, the NMR experiment can provide valuable data on the chemical environment, dynamics, and interaction with other molecules in solution. The application of 2-D NOESY to the determination of protein structure is generally far more complex than for DNA, mainly because the irregular structure of proteins does not allow resonance assignments to be made on the basis of a NOESY spectrum alone. For example, if a cross peak between an amide (in the 8-ppm region) and a C_α proton (in the 4-ppm region) is observed, it is impossible to predict whether it arises from two

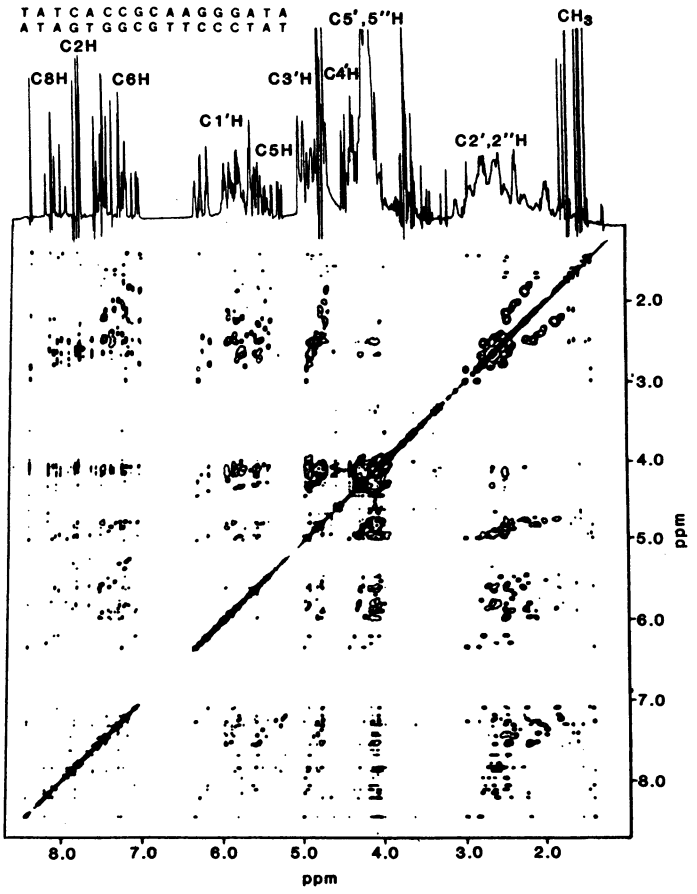

Fig. 4. Absorption mode 2-D NOE spectrum of the OR3 operator DNA fragment, a DNA oligomer of 17 base pairs, recorded at 500 MHz. A mixing time of 200 msec was used; total measuring time was approximately 17 hours. The conventional ^{1}H spectrum is shown along the top. Each of the several hundred resolvable off-diagonal peaks corresponds to a pair of neighboring protons. The coordinates of the peak are the chemical shifts of the two protons, and its intensity is a function of the distance between them. Details of the interpretation are given by Wemmer *et al.* (*11*). The spectrum was provided by B. Reid and G. Drobny.

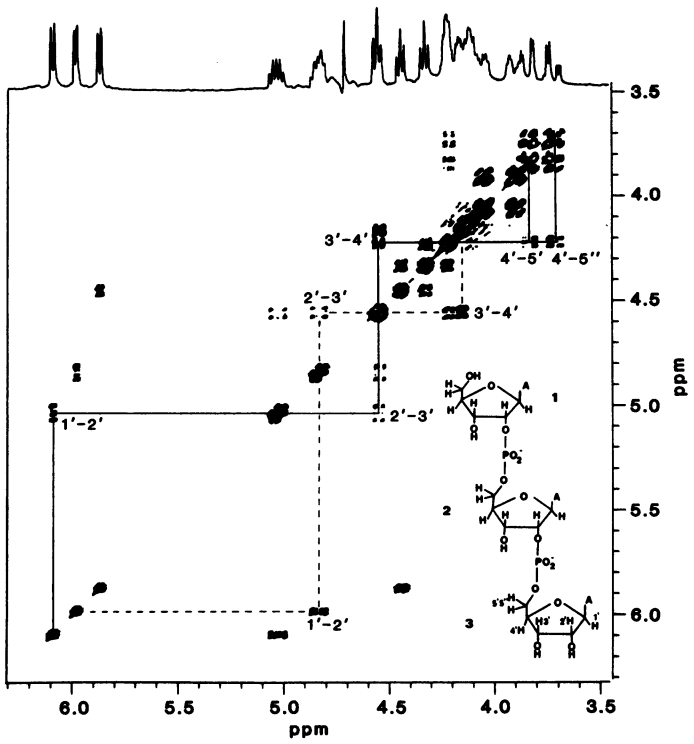

Fig. 5. Double-quantum filtered absorption mode (270 MHz) 2-D COSY spectrum of the ribose region of the trinucleotide A2′-P-5′A2′-P-5′A, with the conventional ^{1}H spectrum shown along the top axis. The solid lines indicate connectivity within the sugar ring of nucleotide 1, the broken line is for the sugar ring of 2. The total measuring time for this spectrum was 3 hours. A, adenine.

protons that are on the same amino acid residue or on different residues. Therefore, for a molecule whose approximate conformation is not known in advance, additional experiments are required to obtain the crucial resonance assignment information. Several reviews describe the commonly used strategies for structure determination of proteins by NMR (*17*).

Accuracy of distance information from 2-D NOESY. The accuracy of distances obtained from 2-D NOE spectra is a highly controversial issue. Practical problems are the exact measurement of cross-peak intensities and the fact that Eq. 1 is valid only for short mixing times Δ, which yield low-intensity cross peaks. Another problem occurs if the molecule deviates significantly from the spherical model, in which case a single correlation time τ_c does not suffice to describe its tumbling. A fundamental problem occurs when there is internal mobility within the molecule that is slow compared to τ_c but fast on the NMR time scale. Because of its dependence on r^{-6}, the NOE intensity can yield an apparent interproton distance that is weighted toward small values of r and differs significantly from the actual time average of r. Although for rigid molecules interproton distances may be reliably determined to ± 0.2 Å, for flexible molecules a more conservative estimate may be appropriate. Finally, since the NMR method can measure only relatively short interproton distances, the errors in these measurements can accumulate if one attempts to reconstruct the entire skeleton of a molecule. Fortunately, even if only a limited number of NOE contacts can be found between regions of known secondary structure (for example, between two α-helices), the relative orientations of these fragments can be determined quite accurately. The use of molecular dynamics calculations in combination with the NMR data has been proposed to further refine the NMR structure (*18*).

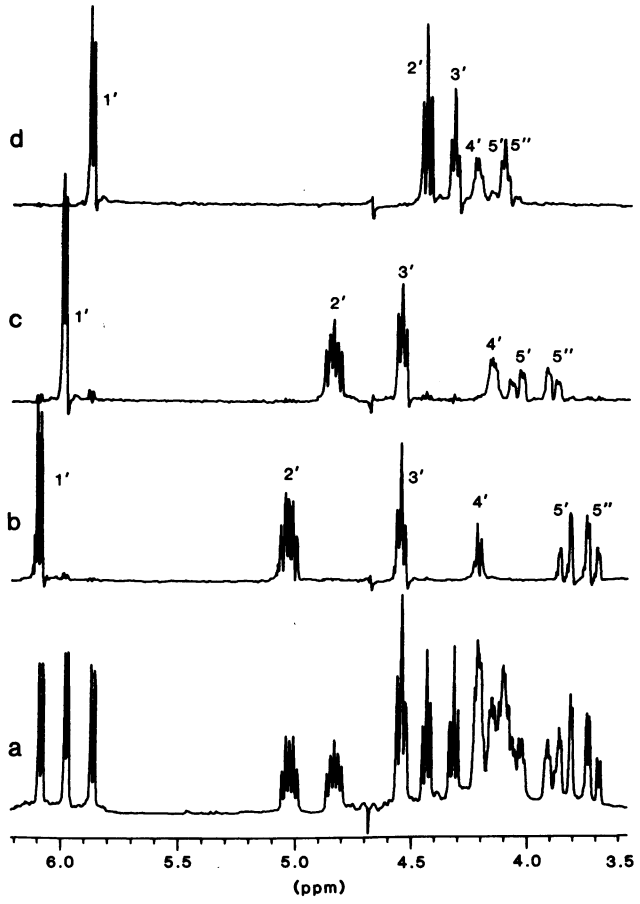

Fig. 6. Spectra of the ribose region of A2′-P-5′A2′-P-5′A (270 MHz). Conventional spectrum (a) and experimental subspectra (b through d) generated with the homonuclear Hartmann-Hahn method, after selective inversion of each anomeric ^{1}H resonance (*31*). The measuring time for each subspectrum was 10 minutes.

Correlation by Homonuclear Scalar Coupling

As mentioned above, the 2-D NOE method alone is not sufficient for obtaining a complete spectral assignment unless the approximate 3-D conformation of the molecule is known. Also, for relatively small molecules (molecular weight <3000) the NOE effect in 2-D NOE spectra is small, so the sensitivity of the method is low. In these cases, a simpler and more sensitive method is to transfer magnetization from one nucleus to another through the scalar coupling mechanism. Jeener's original 2-D experiment (with a sequence of a 90° pulse, then a period t_1, then a 90° pulse, then an acquisition period t_2) was devised for this purpose. If this sequence is applied to a system of homonuclear coupled nuclei (coupled ^{1}H or coupled ^{31}P nuclei), the second 90° pulse in this sequence transfers part of the magnetization from nucleus A to its coupling partner X. In the 2-D spectrum, cross multiplets will be present at frequency coordinates (Ω_A,Ω_X) and at (Ω_X,Ω_A) if and only if nuclei A and X are scalar coupled. Explanation of this magnetization transfer mechanism requires either a density matrix description (*2*), a pulse-cascade description (*19*), or, most conveniently, an operator-formalism description (*20*), all of which fall beyond the scope of this article. The mechanism is most efficient for scalar couplings that are large relative to the line widths of the coupled nuclei. The experiment can also be optimized for detecting the presence of small couplings through four or more bonds, but only at a significant cost in sensitivity (*19*). However, for small organic molecules (molecular weight <500) and adequate sample quantities (>1 mg) this usually does not present a serious limitation, and couplings as small as 0.1 Hz can be observed. The main use, however, of this so-called COSY (COrrelation SpectroscopY) experiment is to determine which pairs of protons are scalar coupled by a two- or three-bond coupling. An example is shown in Fig. 5 for the sugar protons in the trinucleotide A2′-P-5′A2′-P-5′A, a potent inhibitor of protein synthesis. The ribose protons of the three unequivalent sugar rings show severe overlap in the conventional ^{1}H spectrum, recorded at 270 MHz (Fig. 5). The anomeric (C1′) protons resonate the furthest downfield and each has only one coupling partner, the 2′ proton. In the COSY spectrum the position of the 2′ resonance is then found readily because of the cross peak with its corresponding anomeric proton. The connectivity between the 2′ and 3′ protons is also clearly seen, but unfortunately, the ^{1}H multiplets of the 3′ protons of nucleotides 1 and 2 appear at the same frequency. Therefore, it is not possible to determine from this spectrum alone which 4′ resonance corresponds to which nucleotide. The correct connectivity patterns for the ribose rings 1 and 2, confirmed by an experiment to be discussed later, are indicated by solid and broken lines in Fig. 5. This example points to how one would complete the assignment of a set of scalar coupled protons from such a 2-D spectrum. The problem, however, is also clear: if two multiplets exactly overlap in the 1-D spectrum, then a definite assignment cannot be made. For example, because resonances of the 3′ protons of sugars 1 and 2 overlap, assignment of the 4′ and 5′ resonances is ambiguous. A second problem is which set of protons corresponds to which nucleotide.

Partial overlap of spin multiplets is common in ^{1}H NMR spectra, and the highest possible resolution in the 2-D spectrum is needed to resolve such ambiguities. Consequently, the spectra need to be recorded with high digital resolution, which requires large data

matrices and relatively long measuring times. For convenience, 2-D NMR spectra have been commonly presented in the absolute value mode (*19, 21*), which contains contributions from both the narrow absorptive and the broad dispersive components of the line shape. However, it has been demonstrated that in all types of 2-D spectroscopy where resolution is critical, it is important to present the spectra in the absorptive mode (*22*). This approach requires more operator skill to obtain the final 2-D spectrum, but the higher resolution and sensitivity obtained are well worth the effort. In the COSY experiment it was fundamentally impossible to record a pure absorptive 2-D spectrum until a so-called multiple quantum filter was added to the conventional scheme (*23*). The phase characteristics of multiple quantum transitions (those in which more than one nucleus participates simultaneously) are used in this modification to permit the recording of absorptive COSY spectra. In addition, this modification suppresses signals from protons that are not scalar coupled to other protons. Further developments of this multiple quantum filtration procedure allow the selection of particular spin systems and the suppression of all other resonances from the 2-D spectrum. Levitt and Ernst (*24*) have demonstrated that one can record, for example, a COSY spectrum containing only resonances from the alanine residues in a small protein, with resonances from all other amino acids suppressed by the multiple quantum filtration procedure, thus providing dramatic spectral simplification.

Generation of Subspectra

For the case of the trinucleotide, shown in Fig. 5, the three ribose rings form spin systems of identical type, and none of the sophisticated methods mentioned above can provide the complete assignment of this relatively simple molecule. A new technique has been proposed that generates experimental subspectra for each individual sugar ring, providing an unequivocal answer to such assignment problems. The concept of this new technique relies on the principle of isotropic mixing (*25*), and provides the basis of the Hartmann-Hahn experiment (*26*), which is widely used for sensitivity enhancement in solid-state NMR (*27*). The idea of isotropic mixing is to remove the Zeeman terms from the Hamiltonian (*28*) temporarily, either by removal of the sample from the magnetic field (*29*), or more conveniently, by the application of suitable pulse sequences (*30*). Without the presence of the Zeeman interaction between the nuclei and the magnetic field, magnetization diffuses from one proton to the next at rates determined by the size of the scalar couplings (or dipolar couplings, in solids). If, before this isotropic mixing, the magnetization of one particular proton has been inverted by means of a selective 180° pulse, the inverted magnetization will then be redistributed over all protons in the spin system during the subsequent mixing. For example, if the furthest downfield anomeric proton of the trinucleotide is inverted, isotropic mixing will result in attenuated intensities for all protons of that sugar residue. A difference spectrum, obtained by subtracting a spectrum without the selective spin inversion, shows only the attenuated resonances; that is, only the protons of one of the ribose rings (Fig. 6b) (*31*).

The experiment can also be performed in a 2-D fashion (*30, 32*), without selective spin inversion. For complicated spin systems, the 2-D approach is generally preferable for the reasons mentioned earlier for the 2-D NOESY experiment. Again, it is important to record homonuclear Hartmann-Hahn spectra in the absorption mode. Even if the scalar coupling is significantly smaller than the natural line width, this experiment can effectively transfer magnetization between nuclei (*32*). This property makes the method especially useful for the study of connectivity in macromolecules.

Relayed Connectivity Through ^{31}P

Many 2-D NMR experiments are less general in applicability than the methods mentioned above and have been designed specifically for certain types of molecules. For example, in the case of the trinucleotide, it is not obvious which subspectrum in Fig. 6 corresponds to which nucleotide. If magnetization of the 2′ proton of nucleotide 1 could be transferred to the 5′,5″ protons of nucleotide 2, then the subspectra could be assigned with certainty. The long-range scalar coupling between these two protons is much too small to permit the observation of a COSY cross peak, so a different approach is needed. One solution to this problem is to

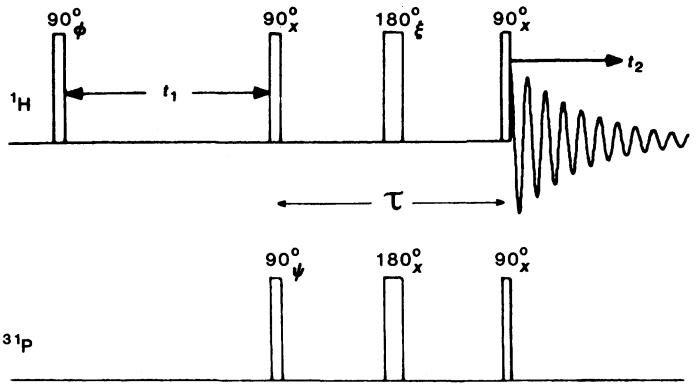

Fig. 7. Pulse sequence of the ^{1}H-^{31}P-^{1}H relay experiment. For each t_1 value, the experiment is repeated 32 times with different phases ϕ, ψ, and ξ of the 90° and 180° pulses, to suppress signals that have not been relayed via ^{31}P. Both ϕ and ψ are cycled along the x, y, $-x$, and $-y$ axes, whereas ξ is cycled along the x and $-x$ axes only. This process of phase cycling simplifies the 2-D spectrum. The fixed duration of τ is chosen to be about $1/3J_{HP}$.

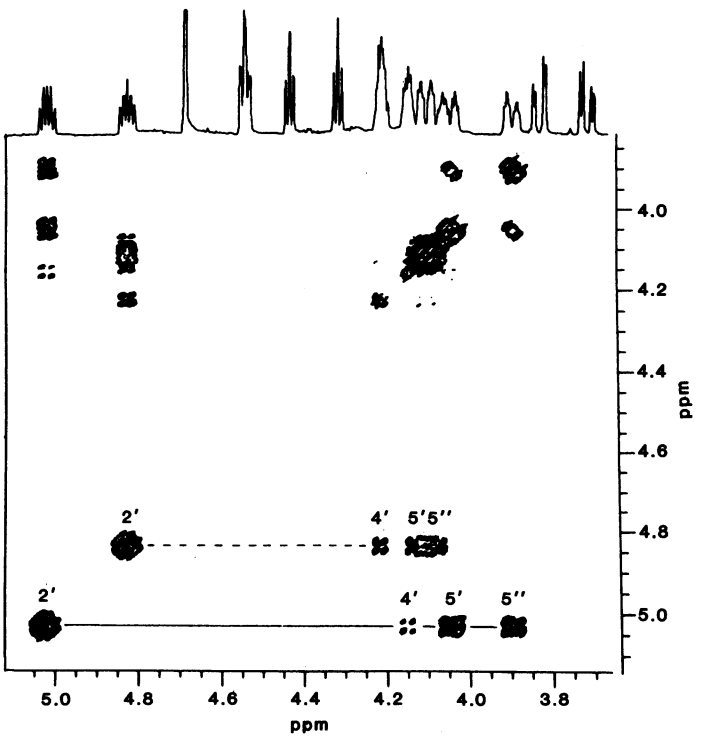

Fig. 8. Absorption mode (500 MHz) ^{1}H-^{31}P-^{1}H relay spectrum of A2′-P-5′A2′-P-5′A. The total measuring time was 6 hours. Connectivities between the 2′ proton of 1 and the 4′, 5′, and 5″ protons of 2 (solid line) and the 2′ proton of 2 and the 4′, 5′, and 5″ protons of 3 (broken line) identify each of the nucleotides.

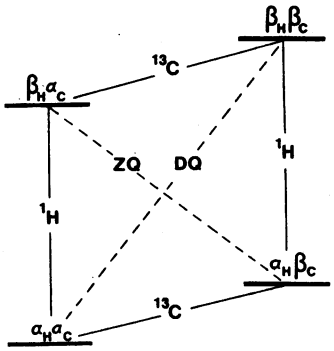

Fig. 9. Energy level diagram of a ^1H-^{13}C spin system. The solid lines indicate directly observable ^1H and ^{13}C transitions. The broken lines indicate zero and double quantum transitions that can only be observed by means of a 2-D experiment.

transfer magnetization first from the 2′ proton to the ^{31}P and then to relay this magnetization to the 5′,5″ protons of the next nucleotide (*33*). The pulse sequence needed for this 2-D experiment is illustrated in Fig. 7. To maximize the transfer of magnetization from the 2′ to the 5′,5″ protons, one must set the time τ between the evolution period (t_1) and detection period (t_2) to about $1/3J_{HP}$, where J_{HP} is the estimated ^1H-^{31}P scalar coupling. This experiment is repeated several times for the same duration of the evolution period but with different RF phases (for example, $0 = x; y, -x$, and $-y$ axes) of the 90° and 180° pulses. When this process of phase-cycling is properly executed, signals that are not transferred via the ^{31}P nucleus can be eliminated, simplifying the 2-D spectrum. Figure 8 shows the 2-D ^1H-^{31}P-^1H relay spectrum of the trinucleotide, demonstrating connectivity from proton 2′ of nucleotide 1 to protons 5′, 5″, and 4′ of nucleotide 2. Similarly, proton 2′ of nucleotide 2 shows connectivity to the 5′, 5″, and 4′ protons of nucleotide 3, completing the assignment of the spectra without ambiguity.

The phase-cycling procedure mentioned above is a critical element of all 2-D experiments. A change in the phase cycling in a particular experiment, with all other parameters unchanged, can completely change the outcome of the experiment. For example, with different phase cycling, the relay experiment of Fig. 7 can be converted into a 2-D NOESY experiment. Many of the current developments in 2-D NMR are related to the construction of better phase cycles (*34*).

Sensitivity-Enhanced Detection of Nuclei with a Low γ

It is a common misconception that 2-D NMR is much less sensitive than 1-D experiments. This idea results partly from negative experiences with nonoptimized 2-D experiments. It is, for example, more critical for sensitivity to optimize the setting of all variables in a 2-D experiment than in its 1-D equivalent. Furthermore, it is not fair to compare, for example, a single 1-D NOESY experiment with a complete 2-D NOESY experiment because one may have to do hundreds of 1-D experiments (if at all feasible) to obtain all the information present in the 2-D experiment. The 2-D experiment is generally more sensitive per unit measuring time if more than about three selective 1-D experiments are required to answer the same question. A more detailed discussion of the sensitivity of 2-D NMR can be found elsewhere (*35*).

For the detection of low-γ nuclei such as ^{15}N and ^{13}C, a suitable 2-D experiment may be an order of magnitude more sensitive than a 1-D experiment. In addition, the 2-D experiment will provide a wealth of extra information not present in the 1-D experiment. Here we focus on the case of a proton, directly coupled to a ^{13}C nucleus. The energy level diagram (Fig. 9) in this case consists of four levels, corresponding to the αα, αβ, βα, and ββ spin states for each coupled ^1H-^{13}C pair, where α and β indicate whether the nucleus is parallel or antiparallel to the static magnetic field. The ^{13}C transitions occur around a frequency that is approximately one-fourth that of protons, and sensitivity is therefore lower by about a factor of 60 (for the same number of nuclei). A common 2-D experiment is an indirect observation of the effect of the proton transitions on the ^{13}C intensities. This results in a so-called heteronuclear shift correlation spectrum with the ω_2 coordinate equal to the ^{13}C chemical shift, and the ω_1 coordinate equal to the chemical shift of the proton or protons directly attached to this ^{13}C nucleus (*36*).

A more sensitive approach is to observe the effect of the ^{13}C nuclei on the protons. Indirect observation of an insensitive nucleus (that is, with a low γ) by its effect on a sensitive nucleus (or electron) has a long history in NMR and electron spin resonance (ESR). However, a major obstacle to this approach is the low natural abundance of ^{13}C (1.1 percent); consequently, most protons will not be modulated by the ^{13}C signal. Although the signals from protons not coupled to ^{13}C could be eliminated by suitable phase cycling, complete suppression of these intense, unwanted signals remained too difficult a practical problem to use this method routinely. This situation changed when the experiment was modified to measure the multiple quantum transitions between the levels αα-ββ and αβ-βα (Fig. 9), instead of the ^{13}C frequency indirectly. The double quantum frequency for the αα-ββ transition occurs at the sum of ^1H and ^{13}C chemical shift frequencies, and it is not directly observable in 1-D NMR. However, the transition can be created easily and its effect monitored indirectly in a 2-D experiment (*37*). The computer can

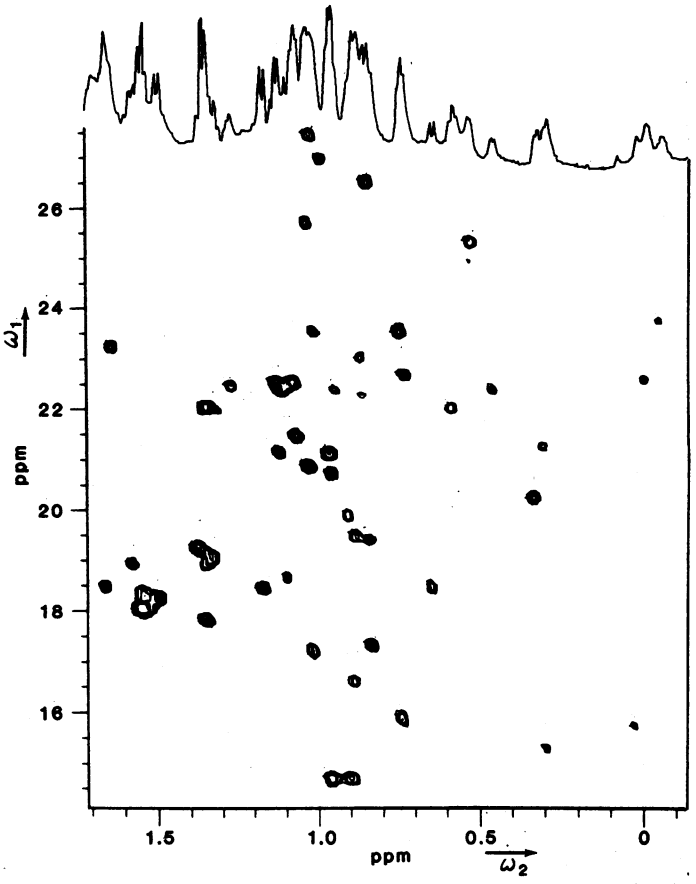

Fig. 10. Absorption mode ^1H-^{13}C shift correlation spectrum of the methyl region of a 25-mg sample of hen egg white lysozyme, dissolved in 0.25 ml of D_2O, at 40°C. The spectrum was obtained by a multiple quantum method, and the total measuring time was 3.3 hours. The ω_2 coordinate of a peak is the ^1H frequency of a particular methyl group and the ω_1 coordinate is the corresponding ^{13}C frequency.

modify such a multiple quantum spectrum to display it in the conventional mode, with the ^1H shift along the ω_2 axis and the shift of its directly coupled ^{13}C nucleus along the ω_1 axis. Figure 10 shows an example of such a spectrum for the methyl region of lysozyme, a relatively small enzyme with a molecular weight of 14,600. The measuring time for this spectrum was only 3 hours. Methyl groups are particularly sensitive to detection this way, not only because of their favorable relaxation properties but also because three protons are used to detect the resonance of a single ^{13}C nucleus, which enhances the sensitivity of the method by an extra factor of 3. Recording of such a ^1H-^{13}C connectivity map removes overlap in both the ^1H and ^{13}C spectra, and thus provides a powerful approach to study the effect of amino acid substitutions and ligand binding on both ^1H and ^{13}C chemical shifts, a potentially useful and versatile method to study protein structure and function (*38*).

Indirect detection of the low-γ nucleus is even more beneficial for ^{15}N spectroscopy, where sensitivity enhancement factors of up to 100 can be obtained experimentally (*39*). The equipment needed for such experiments has more requirements than that for direct observation: spectrometer stability requirements are very high, at least for samples at natural abundance, and the dynamic range problem (*40*) is much more severe than for direct detection of the low-γ nucleus. Improvements in spectrometer hardware are expected to alleviate these problems significantly, and the potential gain in sensitivity will certainly be worth the effort. With this method, 2-D ^1H-^{13}C shift correlation spectra of organic molecules of molecular weight M can be recorded on as little as M micrograms of material in an overnight experiment. The multiple quantum shift correlation method has also proven successful for the study of other heteronuclei, and interesting applications to ^{113}Cd NMR have been reported recently (*41*).

Conclusions

The 2-D approach enormously broadens the applicability of NMR to the study of complex chemical problems. In addition to their application to the proteins and nucleic acids cited in this article, 2-D NMR techniques are being applied to questions of structure and function for an ever-increasing number of other types of molecules, such as peptides (*42*), natural products (*43*), oligosaccharides (*44*), and synthetic polymers (*45*). Two-dimensional NMR simplifies spectral analysis by spreading out information in two frequency dimensions and by revealing interactions between nuclei. Only a few typical experiments of the large collection available have been discussed here, and the development of new experimental techniques continues. Particularly rapid growth is occurring in the area of multiple quantum 2-D NMR, improving spectral simplification and sensitivity even more. Although the mechanisms on which the various pulse sequences rely may be intricate, the interpretation of 2-D NMR spectra is usually straightforward and should therefore not deter the interested chemist. The most important limitation now appears to be the amount of expensive NMR instrument time that is required for the study of complex problems by 2-D NMR. Despite this expense, modern high-resolution multipulse NMR is one of the fastest growing branches of spectroscopy used in chemistry and biochemistry today.

REFERENCES AND NOTES

1. J. Jeener, Ampère International Summer School, Basko Polje, Yugoslavia (1971), unpublished lecture.
2. W. P. Aue, E. Bartholdi, R. R. Ernst, *J. Chem. Phys.* **64**, 2229 (1979).
3. A. Kumar, D. Welti, R. R. Ernst, *J. Magn. Reson.* **18**, 69 (1975).
4. P. C. Lauterbur, *Nature (London)* **242**, 6528 (1973).
5. L. Müller, A. Kumar, R. R. Ernst, *J. Chem. Phys.* **63**, 5490 (1975); G. Bodenhausen *et al.*, *ibid.* **65**, 839 (1976); W. P. Aue, *et al.*, *ibid.*, p. 4226.
6. R. Freeman and G. A. Morris, *Bull. Magn. Reson.* **1**, 5 (1979); R. Freeman, *Proc. R. Soc. London Ser. A* **373**, 149 (1980); A. Bax, *Two-Dimensional Nuclear Magnetic Resonance in Liquids* (Reidel, Boston, 1982); R. Benn and H. Günther, *Angew. Chem. Int. Ed. Engl.* **22**, 350 (1983); P. H. Bolton, in *Biological Magnetic Resonance*, L. Berliner and J. Reuben, Eds. (Plenum, New York, 1984), vol. 6, chap. 1; A. Bax, *Bull. Magn. Reson.* **7**, 167 (1985).
7. T. C. Farrar and E. D. Becker, *Pulse Fourier Transform Nuclear Magnetic Resonance* (Academic Press, New York, 1971), chap. 1.
8. J. Jeener, B. H. Meier, P. Bachmann, R. R. Ernst, *J. Chem. Phys.* **71**, 4546 (1979); S. Macura and R. R. Ernst, *Mol. Phys.* **41**, 95 (1980).

8a. R. S. Balaban and J. A. Ferretti, *Proc. Natl. Acad. Sci. U.S.A.* **80**, 1241 (1983).

9. A. Bax, N. M. Szeverenyi, G. E. Maciel, *J. Magn. Reson.* **52**, 147 (1983); A. Bax, N. M. Szeverenyi, G. E. Maciel, *ibid.* **55**, 494 (1983).
10. J. H. Noggle and R. E. Schirmer, *The Nuclear Overhauser Effect* (Academic Press, New York, 1971).
11. D. E. Wemmer, S.-H. Chou, B. R. Reid, *J. Mol. Biol.* **180**, 41 (1984).
12. R. M. Scheek, N. Russo, R. Boelens, R. Kaptein, *J. Am. Chem. Soc.* **105**, 2914 (1983); D. R. Hare, D. E. Wemmer, S.-H. Chou, G. Drobny, B. R. Reid, *J. Mol. Biol.* **171**, 319 (1983).
13. P. A. Mirau and D. R. Kearns, *Biochemistry* **23**, 5439 (1984); J. Cohen, B. Borah, A. Bax, *Biopolymers* **24**, 747 (1985).
14. D. E. Wemmer, S.-H. Chou, D. R. Hare, B. R. Reid, *Biochemistry* **23**, 2262 (1984); J. Feigon, W. Leupin, W. A. Denny, D. R. Kearns, *ibid.* **22**, 5943 (1983); C. A. G. Haasnoot, H. P. Westerink, G. A. van der Marel, J. H. van Boom, *J. Mol. Biol.* **171**, 319 (1983); M. A. Weiss, D. J. Patel, R. T. Sauer, M. Karplus, *Proc. Natl. Acad. Sci. U.S.A.* **81**, 130 (1984); G. M. Clore, H. Lauble, T. A. Frenkiel, A. M. Gronenborn, *Eur. J. Biochem.* **145**, 629 (1984).
15. A. Kumar, G. Wagner, R. R. Ernst, K. Wüthrich, *Biochem. Biophys. Res. Commun.* **96**, 1156 (1980); G. Wagner, A. Kumar, K. Wüthrich, *Eur. J. Biochem.* **114**, 375 (1981); M. Billiter, W. Braun, K. Wüthrich, *J. Mol. Biol.* **155**, 321 (1982).
16. E. R. P. Zuiderweg, R. Kaptein, K. Wüthrich, *Proc. Natl. Acad. Sci. U.S.A.* **80**, 5837 (1983); F. J. M. van de Ven, S. H. de Bruin, C. W. Hilbers, *FEBS Lett.* **169**, 107 (1984); P. L. Weber, D. E. Wemmer, B. R. Reid, *Biochemistry* **24**, 4553 (1985); T. F. Havel and K. Wüthrich, *J. Mol. Biol.* **182**, 281 (1985); M. P. Williamson, T. F. Havel, K. Wüthrich, *ibid.*, p. 295; A. D. Kline and K. Wüthrich, *ibid.* **183**, 503 (1985).
17. D. E. Wemmer and B. R. Reid, *Annu. Rev. Phys. Chem.* **36**, 105 (1985); K. Wüthrich, G. Wider, G. Wagner, W. Braun, *J. Mol. Biol.* **155**, 311 (1982); F. J. M. van de Ven, thesis, Katholieke Universiteit Nijmegen, The Netherlands, 1985.
18. R. Kaptein, E. R. P. Zuiderweg, R. M. Scheek, R. Boelens, W. F. van Gunsteren, *J. Mol. Biol.* **182**, 179 (1985).
19. A. Bax and R. Freeman, *J. Magn. Reson.* **44**, 542 (1981).
20. O. W. Sørensen, G. W. Eich, M. H. Levitt, G. Bodenhausen, R. R. Ernst, *Progr. Magn. Reson.* **16**, 163 (1983); K. J. Packer and K. M. Wright, *Mol. Phys.* **50**, 797 (1983); F. J. M. van de Ven and C. W. Hilbers, *J. Magn. Reson.* **54**, 512 (1983).
21. K. Nagayama, A. Kumar, K. Wüthrich, R. R. Ernst, *J. Magn. Reson.* **40**, 321 (1980); A. Bax, R. Freeman, G. A. Morris, *ibid.* **42**, 164 (1981).
22. D. J. States, R. A. Haberkorn, D. J. Reuben, *ibid.* **48**, 286 (1982).
23. U. Piantini, O. W. Sørensen, R. R. Ernst, *J. Am. Chem. Soc.* **104**, 6800 (1982); M. Rance *et al.*, *Biochem. Biophys. Res. Commun.* **117**, 479 (1983).
24. M. H. Levitt and R. R. Ernst, *J. Chem. Phys.* **83**, 3297 (1985).
25. D. P. Weitekamp, J. R. Garbow, A. Pines, *ibid.* **77**, 2870 (1982); P. Caravatti, L. Braunschweiler, R. R. Ernst, *Chem. Phys. Lett.* **100**, 305 (1983).
26. S. R. Hartmann and E. L. Hahn, *Phys. Rev.* **128**, 2042 (1962).
27. A. Pines, M. G. Gibby, J. S. Waugh, *J. Chem. Phys.* **59**, 569 (1973); G. E. Maciel, *Science* **226**, 282 (1984).
28. D. P. Weitekamp *et al.*, *Phys. Rev. Lett.* **50**, 1807 (1983).
29. C. P. Slichter, *Principles of Magnetic Resonance* (Springer-Verlag, Berlin, ed. 2, 1980).
30. D. G. Davis and A. Bax, *J. Am. Chem. Soc.* **107**, 2821 (1985); A. Bax and D. G. Davis, *J. Magn. Reson.* **65**, 355 (1985); L. Braunschweiler and R. R. Ernst, *ibid.* **53**, 521 (1983).
31. D. G. Davis and A. Bax, *J. Am. Chem. Soc.* **107**, 7197 (1985).
32. A. Bax and D. G. Davis, in *Advanced Magnetic Resonance Techniques in Systems of High Molecular Complexity*, N. Niccolai and G. Valensin, Eds. (Birkhauser, Basel, in press).
33. M. A. Delsuc, E. Guittet, N. Trotin, J. Y. Lallemand, *J. Magn. Reson.* **56**, 163 (1984); D. Neuhaus, G. Wider, G. Wagner, K. Wüthrich, *ibid.* **57**, 164 (1984).
34. G. Bodenhausen, H. Kogler, R. R. Ernst, *ibid.* **58**, 370 (1984).
35. M. H. Levitt, G. Bodenhausen, R. R. Ernst, *ibid.*, p. 462.
36. A. A. Maudsley and R. R. Ernst, *Chem. Phys. Lett.* **50**, 368 (1977); G. Bodenhausen and R. Freeman, *J. Magn. Reson.* **28**, 471 (1977); A. Bax, in *Topics in Carbon-13 NMR*, G. C. Levy, Ed. (Wiley, New York, 1984), chap. 8.
37. A. Bax, R. H. Griffey, B. L. Hawkins, *J. Magn. Reson.* **55**, 301 (1985); R. H. Griffey *et al.*, *Proc. Natl. Acad. Sci. U.S.A.* **80**, 5895 (1983); R. H. Griffey *et al.*, *J. Biol. Chem.* **260**, 9734 (1985).
38. J. L. Markley *et al.*, *Fed. Proc. Fed. Am. Soc. Exp. Biol.* **43**, 2648 (1984).
39. A. Bax, R. H. Griffey, B. L. Hawkins, *J. Am. Chem. Soc.* **105**, 7188 (1983); D. H. Live, D. G. Davis, W. C. Agosta, D. Cowburn, *ibid.* **106**, 6104 (1984).
40. E. Fukushima and S. B. W. Roeder, *Experimental Pulse NMR* (Addison-Wesley, Reading, MA, 1981), pp. 79–81.
41. D. H. Live, D. Delgano, I. A. Armitage, D. Cowburn, *J. Am. Chem. Soc.* **107**, 441 (1985); J. D. Otvos, H. R. Engeseth, S. Wehrli, *J. Magn. Reson.* **61**, 579 (1985).
42. H. Kessler *et al.*, *J. Am. Chem. Soc.* **104**, 6297 (1982).
43. D. M. Roll *et al.*, *ibid.* **107**, 2916 (1985); N. S. Bhacca *et al.*, *ibid.* **105**, 7188 (1983).
44. J. H. Prestegard, T. A. W. Koener, Jr., P. C. Demou, R. K. Yu, *ibid.* **104**, 4993 (1982); A. Bax, W. Egan, P. Kovac, *J. Carbohydr. Chem.* **3**, 593 (1984).
45. M. D. Bruch, F. A. Bovey, R. E. Cais, J. H. Noggle, *Macromolecules* **18**, 1253 (1985).

46. We thank E. D. Becker, C. Fisk, R. Freeman, W. Hagins, I. Levin, and A. Szabo for many constructive comments during the preparation of this manuscript. L.L. is supported by an Arthritis Foundation postdoctoral fellowship. The sample of trinucleotide A2′-P-5′A2′-P-5′A (Fig. 5) was provided by P. Torrence.